Eur. Phys. J. A **25**, s01, 83–87 (2005)
DOI: 10.1140/epjad/i2005-06-120-3

EPJ A direct
electronic only

β-decay studies of neutron-rich nuclei

P.F. Mantica[a]

NSCL and Department of Chemistry, Michigan State University, East Lansing, MI 48824, USA

Received: 15 January 2005 /
Published online: 27 June 2005 –

Abstract. Recent results of β-decay studies performed along the expected neutron shell closures at $N = 20$, 28, 50 and 82 are reviewed and discussed in view of the potentially dynamic nature of neutron single-particle states in nuclei having extreme neutron-to-proton ratios.

PACS. 23.40.-s β decay; double β decay; electron and muon capture – 21.10.-k Properties of nuclei; nuclear energy levels

1 Introduction

The advancement of β-decay studies into the so-called "terra incognita" region of the chart of the nuclides promises many rewards associated with both nuclear structure and nuclear astrophysics. The nucleon-nucleon effective interactions employed in current nuclear structure models can be more thoroughly tested by examining variations of gross nuclear properties over a wider range of isospin. Characteristics of β decay, as well as the structure of the resulting daughter nuclei populated following the decay, can shed light on new nuclear structure features that are predicted to occur in nuclei with low neutron separation energies. β-decay half-lives, Q_β values, and delayed neutron emission probabilities of neutron-rich nuclei are also important nuclear physics input parameters for network calculations attempting to reproduce r-process abundances.

In fig. 1 is shown a schematic of the β^--decay process. A variety of measurables are available following β decay, and the properties determined will depend on the arrangement of the experimental apparatus. The determination of $T_{1/2}$ can be achieved by monitoring the decay of the β activity with time. The β-decay Q value can be measured from the β energy spectrum, or by measuring the masses of both the parent and daughter nuclides. Information on the low-energy quantum states in the daughter, as well as branching ratios, can be deduced from delayed γ rays measured in coincidence with β particles. The population of states in the daughter above neutron threshold can be deduced by measuring delayed neutrons in coincidence with β particles. Neutron emission probabilities can also be inferred from γ-ray intensities of A and $A-1$ species further down the decay chain. Lifetimes of order picoseconds to nanoseconds of excited levels in the daughter nucleus can be determined using fast timing coincidence methods. For a collection of parent nuclei that are spin polarized, the β-decay asymmetry can be measured, and used to deduce the static nuclear moments of the β-emitting state.

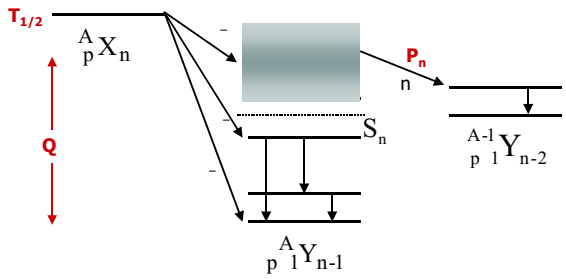

Fig. 1. Schematic of β^- decay.

Significant progress in the study of β-decay properties of very neutron-rich nuclides has been made in recent years, and can be attributed in part to the following: increases in primary beam intensities at radioactive beam facilities; advances in the separation of an isotope of interest from other beam contaminants; and the implementation of new and more sensitive detection methods. In this paper, recent results of β-decay measurements on the neutron-rich side of the valley of stability are detailed. Specific focus is placed on the low-energy nuclear structure of nuclides near the $N = 20$, 28, 50, and 82 neutron closed shells.

2 Island of inversion near N = 20

The weakening of the $N = 20$ shell gap and intrusion of neutron fp orbitals into the sd shell has been well documented for the neutron-rich $_{12}$Mg and $_{11}$Na isotopes with $N \geq 20$ [1,2,3,4,5]. However, details regarding entry into

[a] Conference presenter; e-mail: mantica@msu.edu

the so called "island of inversion" have been sparse. β decay is one method which researchers have used to populate and study the low-energy excited states of the neutron-rich $_{13}$Al, $_{12}$Mg and $_{11}$Na isotopes.

One determination of the entry point into the island of inversion above ^{32}Mg was attempted by Morton *et al.* [6], who measured the β-decay half-life of the $N = 20$ nuclide ^{33}Al. The desired ^{33}Al fragments were produced via fast fragmentation of a ^{40}Ar beam at the National Superconducting Cyclotron Laboratory (NSCL) at Michigan State University. Implanted species were correlated with subsequent β decays on an event-by-event basis using a 1-mm thick double-sided Si microstrip detector [7]. The half-life for the ground state of ^{33}Al was deduced to be 41.7 ± 0.2 ms, and agreed with the results of shell model calculations made in the *sd* shell. Most of the β-decay strength from the ^{33}Al ground state was determined to directly populate the ground state of the ^{33}Si daugther, again in agreement with the *sd* shell model results. Based on the correspondence of the β-decay properties of ^{33}Al with predictions from the *sd* shell model, it was concluded that the ^{33}Al ground state lies mainly outside the island of inversion at $N = 20$.

Morton *et al.* also measured the β-decay half-life of ^{33}Mg to be 90.5 ± 1.5 ms. ^{33}Mg lies inside the island of inversion, and evidence for inversion of the *fp* and *sd* single-particle orbitals was obtained from a study of the β decay of ^{33}Na at ISOLDE [8]. ^{33}Na atoms were produced by proton irradiation of a thick UC target, released from the target at high temperature, and ionized using a surface ionization source. The ionized species were then accelerated, mass separated, and implanted into a collection tape. A plastic scintillator was used for β detection, while large volume Ge detectors were used to measure delayed γ rays. Significant β strength to the ^{33}Mg ground state was deduced. The allowed nature of the ground-state β branch supposes positive parity for the ^{33}Mg ground state. The odd neutron in ^{33}Mg would be expected to reside in the neutron $f_{7/2}$ orbital, which has negative parity. The presence of $1p1h$ excitations at low-energy, due to a weakened $N = 20$ shell gap, was used by Nummela *et al.* to explain the anomalous positive parity ground state of ^{33}Mg.

The weakening of the $N = 20$ shell gap may also lead to the development of shape coexistence at low energy. One experimental signature of the presence of competing shapes at low energy is the appearance of 0^+ states. Nummela *et al.* [9] searched for excited 0^+ states in ^{34}Si, using β decay as a mechanism to access the low-energy structure of this nucleus. The parent ^{34}Al was produced and studied in a similar manner to ^{33}Mg. A γ ray with energy 1193 keV was suggested as a candidate $2_1^+ \rightarrow 0_2^+$ transition, which would position the 0_2^+ state at 2133 keV. An in-beam spectroscopy measurement of ^{34}Si, produced as a radioactive beam and inelastically scattered in a deuteron target, revealed coincidence between an 1193 keV γ-ray transition and the $2_1^+ \rightarrow 0_1^+$ transition with energy 3326 keV [10]. The presence of intruding states in the even-even Si isotopes still remains an open and important question.

While the discussion above focused on entry into the island of inversion from above ^{32}Mg, there have been some attempts to systematically describe the entry pathway with increasing neutron number for the $_{12}$Mg and $_{11}$Na isotopes. The ground magnetic dipole moment of ^{31}Mg has recently been measured, where the β-decay asymmetry from spin-polarized ^{31}Mg nuclei was monitored as a function of an applied radiofrequency field. With $N = 19$, ^{31}Mg borders the island of inversion, and the value of the experimental magnetic moment suggests that the ground state is dominated by $2p2h$ intruder configurations [11,12].

For the Na isotopes, the systematic behavior of the ground state quadrupole moments, again determined by monitoring the β-decay asymmetry from polarized sources of $^{26-31}$Na, show a regular increase away from $Q \sim 0$ mb starting at ^{28}Na$_{17}$ [13]. Especially for ^{30}Na, with $N = 19$, the theoretical treatment of the experimental quadrupole moment is best achieved when considering admixtures of the *pf* shell into the ground state [14]. In a recent measurement at the NSCL, the low-energy structure of ^{27,28,29}Na was studying following the β decay of ^{27,28,29}Ne, respectively. Detailed level schemes have been proposed for all three nuclides, and compared with results from *sd* shell model calculations. The low-energy structure of ^{29}Na is not consistent with *sd* shell model predictions. It is suggested from this study of the neutron-rich Na isotopes that a reduced $N = 20$ shell gap is already evident at $N = 18$ [15].

3 β-decay half-life of ^{42}Si$_{28}$

Advancement of knowledge of a potential weakening of the $N = 28$ shell gap for neutron-rich nuclides has not progressed as rapidly as that around $N = 20$. Early suggestions of increased collectivity at $N = 28$ came from the measured short β-decay half-life and small delayed neutron emission probability of ^{44}S by Sorlin *et al.* [16]. Subsequent Coulomb excitation experiments on ^{44}S and neighboring nuclei also provided evidence for a weakened $N = 28$ shell gap [17,18].

It has taken more than 10 years to get first data for the next even-even nucleus along the $N = 28$ isotonic chain. The half-life of $^{42}_{14}$Si$_{28}$, along with 11 other neutron-rich nuclides of Mg-Ar, were measured for the first time by Grévy *et al.* [19]. The nuclides were produced using fast fragmentation of a 60 MeV/nucleon ^{48}Ca beam at GANIL. The half-life of ^{42}Si was deduced to be $T_{1/2} = 12.5 \pm 3.5$ ms, and comparison with the results of QRPA calculations suggested strong oblate deformation for the ^{42}Si$_{28}$ ground state.

Moving back towards ^{48}Ca, measurement of the gross β-decay properties of the $_{18}$Ar isotopes has now been completed beyond the $N = 28$ closed shell [20]. The half-lives and delayed neutron emission probabilities of ^{49,50}Ar were consistent with QRPA calculations assuming small oblate deformation for the parent and daughter ground states. The decay measurements were carried out at ISOLDE, and proved challenging due to the background attributed

to other short-lived radioactive noble gases extracted simultaneously with singly-charged ^{49,50}Ar from the plasma ion source. By mass selecting doubly-charged ^{49,50}Ar ion species, the experimenters were able to collect decay time and delayed neutron spectra suitable for analysis.

4 Shell closure at N = 34?

The high energy of the first excited 2^+ state in $^{52}Ca_{32}$ [21], compared to neighboring $^{50}Ca_{30}$, provided evidence for possible changes in shell structure above ^{48}Ca. Further investigation of the systematic variation of the 2_1^+ energies of the neutron-rich, even-even Cr isotopes by Prisciandaro *et al.* [22] demonstrated that the unexpected stability at $N = 32$ was not limited to the Ca isotopes at the proton closed shell.

The appearance of a subshell gap at $N = 32$ has been attributed to a shift in the neutron $f_{5/2}$ orbital due to a strong proton-neutron monopole interaction with the proton $f_{7/2}$ orbital [23]. Indeed, a similar monopole shift between the proton $d_{5/2}$ and neutron $d_{3/2}$ orbitals around $A = 30$ contributes to the erosion of the $N = 20$ shell closure.

A more complete picture of the development of the $N = 32$ subshell closure with removal of protons from the $f_{7/2}$ orbital was obtained with the measurement of the energy of the first 2^+ state in ^{54}Ti. γ rays with energies 1002 and 1495 keV were observed following the β decay of ^{54}Sc and by in-beam γ spectroscopy following deep inelastic collisions of ^{48}Ca on ^{208}Pb. [24]. The 1495 keV γ ray was assigned as the $2_1^+ \rightarrow 0_1^+$ transition in ^{54}Ti based on its intensity in both the delayed and in-beam γ-ray spectra. The low-energy states of the even-even, neutron-rich Ti isotopes were well reproduced by shell model calculations using a new pf shell effective interaction labeled GXPF1 [25,26]. These same shell model calculations also predicted that the neutron $f_{5/2}$ orbital should rise significantly above the neutron $p_{1/2}$ orbital when the proton $f_{7/2}$ orbital is unoccupied, leading to the development of an $N = 34$ shell closure for the Ti and Ca isotopes. As evidence for the appearance of an $N = 34$ shell closure, the first 2^+ energy in $^{56}Ti_{34}$ is predicted from the GXPF1 shell model calculations to be similar to that in $^{54}Ti_{32}$.

A subsequent measurement of the first excited 2^+ state in ^{56}Ti via β decay [27] did not lend support to the notion of a shell closure at $N = 34$ for the Ti isotopes. The measurement was carried out at the NSCL, where the ^{56}Sc parent nuclides were produced at a rate of ≈ 3 per minute via fast fragmentation of a ^{86}Kr beam at 140 MeV/nucleon. Several γ rays were observed in the delayed γ-ray spectrum of ^{56}Sc, and three transitions at 690, 1129, and 1161 keV were assigned as depopulating levels in ^{56}Ti. The most intense transition at 1129 keV was tentatively assigned as the $2_1^+ \rightarrow 0_1^+$ transition, meaning that the 2_1^+ state in ^{56}Ti was nearly 400 keV below that predicted by the shell model calculations using the GXPF1 interaction.

Detailed analysis of the delayed γ rays following the β decay of ^{56}Ti [28] provided evidence for the presence of two β-decay states in ^{56}Sc; a low-spin state with a half-life of 35±5 ms, and a high-spin state with half-life 60±7 ms. The existence of high- and low-spin β-decaying states helps explain the complicated allowed decay pattern that was observed for ^{56}Sc. Direct β feeding was deduced to both the ^{56}Ti 0^+ ground state and to a state at 2980 keV, believe to have spin and parity 6^+ based on observations from a complementary in-beam spectroscopy measurement [29]. The existence of isomeric states in the parent nucleus offers unique challenges to β-decay experiments, and is discussed in further detail in the next section.

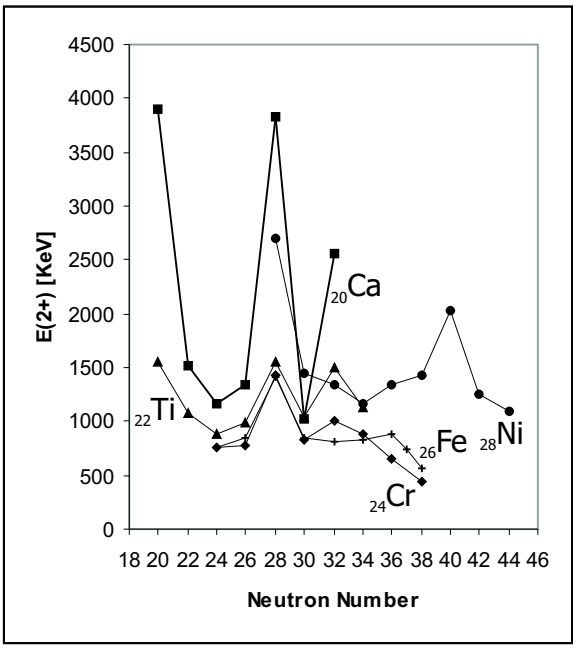

Fig. 2. Systematics of the first 2^+ energies of the proton $f_{7/2}$ neutron fp shell nuclei.

The absence of an $N = 34$ shell closure for the Ti isotopes has been attributed to a less dramatic monopole shift of the neutron $f_{5/2}$ orbital with change in occupancy of the proton $f_{7/2}$ orbital as predicted by the shell model calculations employing GXPF1. A new shell model interaction designated GXPF1a is now under development [30], that may correct some of the observed deficiencies in GXPF1.

The current status of the measured 2_1^+ energies for the Ca to Ni isotopes in the fp shell is shown in fig. 2. The systematic increase in 2_1^+ at $N = 32$ is evident in the $_{20}$Ca, $_{22}$Ti, and $_{24}$Cr isotopes. There is no indication of an increase in the 2_1^+ energy at $N = 34$ for any of the isotopes shown. In fact, there is a dramatic *decrease* in the first 2^+ energy in the $_{24}$Cr and $_{26}$Fe isotopes beyond $N = 34$. The 2_1^+ energies in $^{60}Cr_{36}$ and $^{62}Cr_{38}$ were determined in β-decay experiments by Sorlin *et al.* [31], where the parent isotopes ^{60,62}V were produced following fast fragmentation of a ^{76}Ge beam at 61.8 MeV/nucleon at GANIL. The systematic trend in 2_1^+ energies for Cr and Fe suggests a sudden onset of deformation, which may be traced to the occupancy of the neutron $g_{9/2}$ orbital. A strong monopole interaction is expected between the proton $f_{7/2}$ and neutron $g_{9/2}$ shell model orbitals [32]. Further studies of the low-energy structure of proton $f_{7/2}$ neutron-rich nuclides

out to $N = 40$ are warranted to fully understand the dynamic nature of the neutron single-particle orbitals due to the monopole shift.

5 Towards $^{78}Ni_{50}$

With a full complement of $f_{7/2}$ protons, the $_{28}$Ni isotopes have been extensively studied by a variety of techniques. For the very neutron-rich $^{78}Ni_{50}$, a half-life has been determined for the first time [33]. Eleven ^{78}Ni nuclei were produced following fast fragmentation of a 140 MeV/nucleon ^{86}Kr beam at the NSCL. The half-life deduced for ^{78}Ni was considerably shorter than most early predictions from global nuclear structure models, and further details are available in the contribution to these proceeding by Schatz *et al.* [34].

The systematic variation of the first 2^+ energies in the even-even Ni isotopes have now been determined up to ^{76}Ni. The low-energy levels in ^{72}Ni and ^{74}Ni were determined following β decay of ^{72}Co [35] and ^{74}Co [36], respectively. In both cases the parent nuclides were made by fast fragmentation of a ^{86}Kr beam; the ^{72}Co measurement was completed at GANIL using ancillary γ-ray detectors from EXOGAM, while the ^{74}Co data were collect at the NSCL using detectors from the SeGA array for γ-ray detection. The first excited 2_1^+ state in ^{76}Ni was first determined through observation of the decay of the isomeric 8^+ seniority state, which is produced directly in projectile fragmentation and has a lifetime of several ten's of nanoseconds [37]. The same isomer decay sequence was observed in a subsequent experiment at the NSCL [36].

As mentioned in sect. 4, the presence of multiple β-decaying states in a single nucleus can seriously complicate the interpretation of results from a β-decay experiment. Recently, three β-decaying states have been observed in the nucleus ^{70}Cu [38,39]. Characterization of these three β-decaying states was aided by the selectivity offered by resonance laser ioniziation in an on-line ion source. The ^{70}Cu species were produced by proton induced fission of a UC target, both at ISOLDE and the LISOL facility at Louvain-la-Neuve. The hyperfine structures of the three states β-decaying states are sufficiently different, due to the difference in the spin value of each state, to permit in-source laser spectroscopy to enhance production of any one of the three states. In addition to determining half-lives, β-branching, and competing γ internal transitions, the masses of each β-decaying state were determined using ISOLTRAP [40].

Resonance laser ionization sources provide enhanced efficiencies and reduced backgrounds that will significantly broaden the reach of on-line isotope separators in terms of more available isotopes (including refractory metals) with larger N/Z ratios. The opportunties are well outlined in the next section, as well as elsewhere in these proceedings [41].

6 Shell quenching at N = 82

Dillman *et al.* have deduced the mass of $^{130}Cd_{82}$ from a β-decay endpoint measurement [42]. Here the ^{130}Cd nuclides were produced at ISOLDE using a two-step fission target [43] and efficiently extracted from the on-line ion source using resonant laser ionization. The experimental Q_β value of 8.34 MeV was higher than the predictions of global mass models that do not include quenching of the $N = 82$ shell gap. The authors have suggested this is an indication of shell quenching below $^{132}Sn_{82}$. Another early indication of the potential quenching of the $N = 82$ shell gap has come from the systematic variation of the first excited 2^+ states in the even-even $_{48}$Cd isotopes, where the $E(2_1^+)$ value decreases from 652 keV in ^{126}Cd to 645 keV in ^{128}Cd [44]. Even in $^{131}Cd_{83}$, the short half-life and low delayed neutron probability for this nuclide did not compare favorably to theoretical predictions [45].

Additional β-decay studies of the very neutron-rich Sn isotopes have also been carried out at the high resolution mass separator at ISOLDE. Delayed γ-ray spectroscopy has been completed out to $^{135}Sn_{85}$ [46]. A significant decrease in the energy difference between the lowest energy $7/2^+$ and $5/2^+$ levels has been observed in the Sb_{51} isotopes at $^{135}Sb_{84}$. To investigate the origin of this dramatic change in low-energy structure, which might be associated with the large N/Z ratio of ≈ 1.6 in ^{135}Sb, the lifetime of the first excited $5/2^+$ state was measured [47] using the $\beta\gamma\gamma$(t) method with fast timing plastic scintillator and BaF_2 detectors [48]. The lifetime of the $5/2^+$ state in ^{135}Sb was much longer than predicted by shell model calculations using interactions which include the most recent data on nearby ^{133}Sb and ^{133}Sn.

Further removed from ^{132}Sn, neutron-rich nuclides in the Tc-Cd isotopes have been produced by fast fragmentation of a 120 MeV/nucleon ^{136}Xe beam and studied by both delayed γ-ray and delayed neutron spectroscopies. The low-energy structure of ^{120}Pd has been deduced from the delayed γ rays observed following the β decay of ^{120}Rh [49]. The most intense γ-ray transition at 438 keV was assigned to the $2_1^+ \rightarrow 0_1^+$ transition in ^{120}Pd. The systematic variation of the 2_1^+ energies in the $_{46}$Pd isotopes show a symmetry about $N = 68$, where the 2_1^+ energy of ^{108}Pd is reported as 434 keV. In addition, there is also similarity in the first 2^+ energies of the four proton hole $^{120}_{46}Pd_{74}$ and isotonic $^{128}_{54}Xe_{74}$, which has four proton particles outside $Z = 50$. The conclusion reached is that, from a valence-particle standpoint, both $^{128}Xe_{74}$ and $^{120}Pd_{74}$ appear to see the same $N = 82$ and $Z = 50$ shell closures.

Both $^{130}Cd_{82}$ and $^{135}Sb_{84}$ exhibit anomalous properties near the ground state that may be attributed to the extreme N/Z ratio of these nuclides. Continued investigations of the β-decay properties and low-energy structure of nuclides along $N = 82$ may help to confirm or refute the quenching of this shell gap.

7 Summary

Allowed β decay is a selective process, and provides a means to access excited states of nuclei far from stability. Measured and deduced properties that can be obtained by studying β decay include: half-lives, decay energies,

absolute branching ratios, delayed neutron probabilities, as well as low-energy structure of daughter nuclide(s).

New β-decay data for very neutron-rich nuclides have been obtained at both isotope separation on-line ion source and fragmentation facilities. The use of resonance laser ionization has broadened the reach of on-line ion source experiments, providing access to new elements with a high degree of selectivity. The characterization of fast fragmentation beams on an event-by-event basis and direct implant-β correlation methods have allowed first study of ^{78}Ni and other far off stability nuclides.

Future enhancements in selectivity, detector sensitivity, and rare isotope beam production over the near term will provide new data on the β-decay properties of neutron-rich nuclides to learn more of the dynamic nature of single-particle states in nuclides far from the valley of stability.

This work was supported in part by the National Science Foundation PHY-01-10253.

References

1. T. Motobayashi *et al.*, Phys. Lett. B **346**, 9 (1995).
2. B.V. Pritychenko *et al.*, Phys. Lett. B **461**, 322 (1999).
3. V. Chiste *et al.*, Phys. Lett. B **514**, 233 (2001).
4. Y. Yanagisawa *et al.*, Phys. Lett. B **566**, 84 (2003).
5. B.V. Pritychenko *et al.*, Phys. Rev. C **63**, 011305R (2000).
6. A.C. Morton *et al.*, Phys. Lett. B **544**, 274 (2002).
7. J.I. Prisciandaro *et al.*, Nucl. Instrum. Methods Phys. Res. A **505**, 140 (2003).
8. S. Nummela *et al.*, Phys. Rev. C **64**, 054313 (2001).
9. S. Nummela *et al.*, Phys. Rev. C **63**, 044316 (2001).
10. N. Iwasa *et al.*, Phys. Rev. C **67**, 064315 (2003).
11. M. Kowalska *et al.*, these proceedings.
12. G. Neyens *et al.*, Phys. Rev. Lett. **94**, 022501 (2005).
13. M. Keim, *ENAM98, Exotic Nuclei and Atomic Masses*, edited by B.M. Sherrill, D.J. Morrissey, C.N. Davids (AIP, Woodbury, 1998) p. 50.
14. Y. Otsuno *et al.*, Phys. Rev. C **70**, 044307 (2004).
15. V. Tripathi *et al.*, these proceedings.
16. O. Sorlin *et al.*, Phys. Rev. C **47**, 2941 (1993).
17. H. Scheit *et al.*, Phys. Rev. Lett. **77**, 3967 (1996).
18. T. Glasmacher *et al.*, Phys. Lett. B **395**, 163 (1997).
19. S. Grévy *et al.*, Phys. Lett. B **594**, 252 (2004).
20. L. Weissman *et al.*, Phys. Rev. C **67**, 054314 (2003).
21. A. Huck *et al.*, Phys. Rev. C **31**, 2226 (1985).
22. J.I. Prisciandaro *et al.*, Phys. Lett. B **510**, 17 (2001).
23. T. Otsuka *et al.*, Phys. Rev. Lett. **87**, 082502 (2001).
24. R.V.F. Janssens *et al.*, Phys. Lett. B **546**, 55 (2002).
25. M. Honma *et al.*, Phys. Rev. C **65**, 061301R (2002).
26. M. Honma *et al.* Phys. Rev. C **69**, 034335 (2004).
27. S.N. Liddick *et al.*, Phys. Rev. Lett. **92**, 072502 (2004).
28. S.N. Liddick *et al.*, Phys. Rev. C **70**, 064303 (2004).
29. B. Fornal *et al.*, Phys. Rev. C **70**, 064304 (2004).
30. M. Honma *et al.*, these proceedings.
31. O. Sorlin *et al.*, Eur. Phys. J. A **16**, 55 (2003).
32. A.M. Oros-Peusquens, P.F. Mantica, Nucl. Phys. A **669**, 81 (2000).
33. P. Hosmer *et al.*, Phys. Rev. Lett. **94**, 112501 (2005).
34. H. Schatz *et al.*, these proceedings.
35. M. Sawicka *et al.*, Phys. Rev. C **68**, 044304 (2003).
36. C. Mazzocchi *et al.*, these proceedings.
37. M. Sawicka *et al.*, Eur. Phys. J. A **20**, 109 (2004).
38. J. VanRoosbroeck *et al.*, Phys. Rev. Lett. **92**, 112501 (2004).
39. J. VanRoosbroeck *et al.*, Phys. Rev. C **69**, 034313 (2004).
40. F. Herfurth *et al.*, J. Phys. B **36**, 931 (2003).
41. P. van Duppen *et al.*, these proceedings.
42. I. Dillman *et al.*, Phys. Rev. Lett. **91**, 162503 (2003).
43. J.A. Nolen *et al.*, AIP Conf. Proc. **473**, 477 (1999).
44. T. Kautszch *et al.*, Eur. Phys. J. A **9**, 201 (2000).
45. M. Hannawald *et al.*, Phys. Rev. C **62**, 054301 (2000).
46. J. Shergur *et al.*, Phys. Rev. C **65**, 034313 (2002).
47. A. Korgul *et al.*, these proceedings.
48. H. Mach *et al.*, Nucl. Phys. A **523**, 197 (1991).
49. W.B. Walters *et al.*, Phys. Rev. C **70**, 034314 (2004).